



## Design of laser melting of tool steel for surface integrity enhancement

Fazliana Fauzun <sup>1</sup>, Syarifah Nur Aqida Syed Ahmad <sup>2,\*</sup>, Izwan Ismail <sup>3</sup>

<sup>1</sup> Faculty of Mechanical Engineering, Universiti Malaysia Pahang, 26600, Pekan, Pahang, MALAYSIA.

<sup>2</sup> Automotive Excellence Centre, Universiti Malaysia Pahang, 26600, Pekan, Pahang, MALAYSIA.

<sup>3</sup> Faculty of Manufacturing Engineering, Universiti Malaysia Pahang, 26600, Pekan, Pahang, MALAYSIA.

\*Corresponding author: aqida@ump.edu.my

KEYWORDS	ABSTRACT
Laser melting Nd:YAG laser H13 tool steel Response surface methodology Thermal wear resistance	In this study, laser surface modification has been conducted on AISI H13 tool steel for enhance surface properties. A maximum 300 W high power Nd:YAG laser system with pulse mode was used to modify both materials sample surface. Laser processing was conducted using a 3 <sup>3</sup> full factorial design. Three controlled parameters were laser peak power, pulse repetitive frequency (PRF) and scanning speed. The modified surface was characterized for metallographic study, surface morphology and hardness properties. The results showed that finer grain formation occurred at laser modified layer. Grain size decreased along the cross-section of the melted pool, which consequently increased the hardness due to grain refinement. The overlap increased significantly with decreasing laser scanning speed which affected sample surface integrity. Low surface roughness obtained at the highest scanning speed, low peak power and PRF. Process optimization was carried out for maximum surface hardness and laser modified depth, and minimum surface roughness. These findings indicate potential application of tool steel for thermal wear resistant applications through laser surface modification.

Received 1 July 2018; received in revised form 20 September 2018; accepted 12 January 2019.

To cite this article: Fauzun et al. (2019). Design of laser melting of tool steel for surface integrity enhancement. Jurnal Tribologi 22, pp.18-31.

## 1.0 INTRODUCTION

Failures in casting processing have been observed for years. Cyclic high temperature condition and exposure to high viscosity molten metal were among the causes of die to wear and crack. Thermal fatigue caused heat checking which one of most important life-timing tool failure mechanisms in molten metal die casting. These die surface cracks caused unwanted marks or fins on the castings surface thus affected the quality of end products. Many works have been conducted to prolong the die includes high technology coating application and producing superior properties bulk material. However, it is difficult to meet the effective coating requirement which includes excellent bonding, adequate thickness and absence of flaws, suitable mechanical properties, thermal shock resistance and high temperature stability (Batista, Portinha et al. 2005). Besides, when it concerns wear properties, surface modification is preferable.

Among numerous methods of surface modification laser treatment drawn attention because of its unique advantages ( Jae-Ho et al. 2009). Over the past few years, laser surface treatment has been a way to overcome premature failure in casting by developing amorphous layer on die surface (Hassanein et al. 2010). Rapid development in surface engineering field leads to utilization of advanced heat source such as plasma, laser, ion, and electron (Aqida et al. 2012). Tool and die industries pay attention to the technology of laser surface treatment due to its precision of operation, short processing time and localized treatment effects (Yilbas et al. 2009).

Laser heating produced local changes at the surface of the material whilst thus leaving the properties of bulk of a given component unaffected. Laser surface melting (LSM) technique has been widely used to improve surface properties of alloys for improving hardness, corrosion and wear properties (Yasavol et al. 2013). Localise heat treatment method produced surface with controlled surface roughness and profile. Demand from the industry to produce low surface roughness as finishing surface with 5  $\mu\text{m}$  gives laser treatment advantages. Numbers of different laser sources such as Nd:YAG (Neodymium:Yttrium-aluminium-garnet), CO<sub>2</sub> (carbon dioxide), fibre laser and HPDL (High Power Direct Diode) laser system have been widely studied. The wavelengths of these lasers are between 800 and 10,600 nm which offers better light absorption at shorter the wavelength (Jiang et al. 2011).

Surface heat treatment with laser beam experienced self-quenching that cooled rapidly into materials without cooling agent. In laser surface modification of tool steels, rapid solidification produced finer grains which increased hardness properties Majumdar et al. 2010, Roy et al. 2017). Hot work tool steel of H13 was used in precision molds by manufacturing tools for processing or various dies since it has advantages of high resistance to thermal shock, thermal fatigue, abrasion resistance and heat resistant ( Jae-Ho et al. 2009).

The design of experiment (DOE) is important in providing the optimal performance and to quantify the influence of selected parameters. Statistical analysis refers to a collection of methods used to process large amount of data and report overall trends. Various methods such as Response surface method (RSM), Taguchi method, orthogonal experiment design and dynamic neighbourhood-particle swarm optimization (DN-PSO) have been used to overcome the relationship between parameters and optimization of laser processing (Zhang et al., 2010; Bhushan, 2013 and Teixidor et al., 2013). RSM find the ideal process settings to achieve optimal performance and useful for modelling and analysing problems (Aggarwal et al., 2008; Abhang and Hameedullah, 2010; Bhushan, 2013 and Rostami et al., 2014).

Previous researcher proved RSM offers better prediction on the effect of parameters on multi response and optimization compared to Taguchi's technique. 3D surface plot generated by RSM can help in visualizing the effect parameter on response in the entire or across range specified

(Hasran et al., 2013 and Bhushan, 2013). According to Abhang and Hameedullah (2010), RSM was found to be successful technique to perform trend analysis with respect to various combinations of design variables. The models developed produced significant small errors and contour plots which helped designers to select the best combination for optimization process. While Aggarwal (2008) found that analysis of RSM and Taguchi methodology had similar results of power consumption. The objective of this study was designing experiment of AISI H13 tool steel laser melting for enhanced hardness properties with low surface roughness and thick modified layer range from 100 to 300  $\mu\text{m}$  using Nd:YAG laser system.

## 2.0 EXPERIMENTAL PROCEDURE

As-received AISI H13 tool steel of 10 mm thickness was processed and analyzed in this study. Each setting processed a rectangular area of 30 x 50 mm dimension. Chemical composition of AISI H13 tool steel in Table 1 was analyzed using OXFORD INSTRUMENT Foundry-Master spectroscopy. An Nd:YAG JK300HPS laser system with TEM<sub>00</sub> mode was used to process the sample surface with average laser power of 300 W. The smallest laser spot size was 0.6 mm at focal length of 160 mm. The maximum laser scanning speed was 900 mm/min while pulse repetition frequency was 1000 Hz. During the processing, sample was stationary while laser head was translated linearly by CNC motion control system. The laser processing was conducted using pulse mode in an inert argon atmosphere at 1.5 bar to avoid oxidation.

Table 1: Chemical composition of AISI H13 tool steel

Element	C	Si	Cr	Ni	Al	Cu	V	Mo	Fe
wt%	0.401- 0.473	0.968- 1.00	4.92- 5.03	0.073- 0.107	0.024- 0.046	0.08- 0.165	0.901- 0.927	1.78	Balance

A full factorial design of experiment (DOE) of 3<sup>3</sup> was developed and yields 27 parameter settings. Controlled parameters were peak power (P<sub>p</sub>), pulse repetition frequency (PRF) and scanning speed (v). Three responses were depth of modified surface, surface roughness and hardness. The factors and factors levels are summarized in Table 2. Duty cycle was calculated to shorten pulse width thus controlled interaction time between material surface and laser beam. Parameters were set to produce significant amount of energy of 1.7, 2.0 and 2.5 J to melt the sample surface.

Table 2: Factors and factor levels.

Parameter	Low	High
P <sub>p</sub>	1700 W	2500 W
PRF	40 Hz	60 Hz
V	16.67 mms <sup>-1</sup>	23.33 mms <sup>-1</sup>

Modified layer thickness was measured using IM7000 Series Inverted Optical microscopes with Progress Capture 28.8 Jenoptik Optical System image analyzer software. The modified surface roughness was determined using 2D stylus profilometer. Hardness properties were measured using MMT Matsuzawa Vickers Hardness tester with 10 kgf load. Experimental results were statistically analyzed by ANOVA approach to establish relationship between factors and responses.

### 3.0 RESULTS AND DISCUSSION

#### 3.1 Hardness Properties

High power laser beam heats steel surface at almost 1500 °C. Short pulse and high scanning speed affect the most for cooling rates. High cooling rates at short interaction time produced high hardness of modified layer. High energy emitted on steel surface experienced higher temperature while processed at short pulse thus generated a higher hardness layer ( Hua et al. 2009). Localize heating at very short time transmitted full energy on the surface thus produced finer grains formations on melted pool as shown in FE SEM micrographs in Figure 1. In previous work, nano and ultrafine grain size were produced in the modified surface due to large undercooling produced from laser processing (Aqida, Naher et al. 2011). Reduced in particle sizes give great influence to hardness due to stronger bonding between particles.

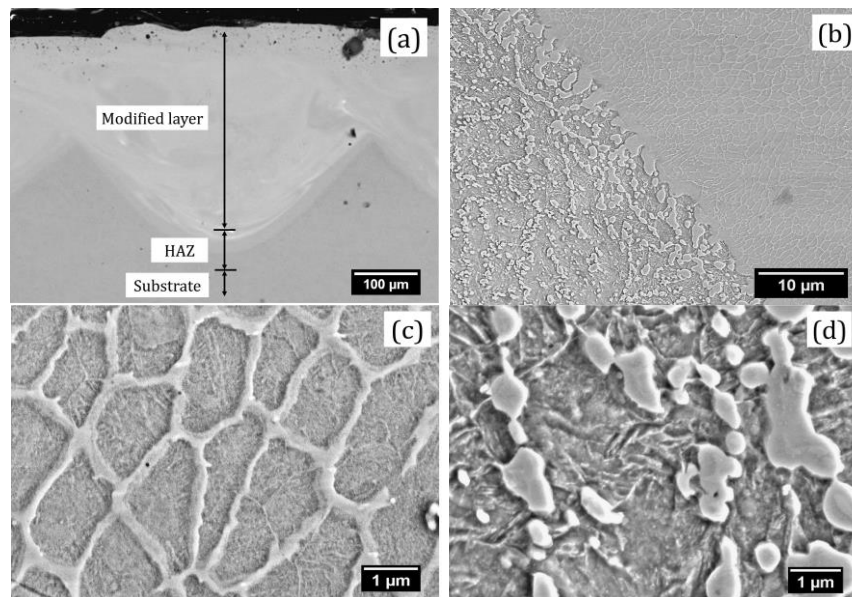


Figure 1: FE SEM micrograph of regions label as (a) modified layer, (b) HAZ area, focused (c) modified grain structure and (d) substrate.

Changes of laser power varied surface heating and cooling rates, thus resulting in different grain sizes in the modified layer surface and heat affected zone. During laser processing, thermal conduction occurred on steel surface by transported the heat away produced by laser beam thus resulted in induction rapid cooling. The properties of modified layer were controlled by the amount of energy input depending on laser power density and interaction time. Cooling rate at different level of molten pool depends on the amount of energy that travels into substrate. Overlapped laser spot caused double heating on the top region of melted pool thus increased the cooling time. Figure 2 shows the schematic diagram on cooling rate of overlapped laser spots.

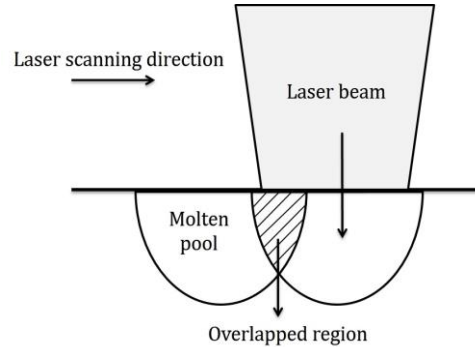


Figure 2: The schematic diagram on cooling rate of overlapped laser spots.

FE SEM micrograph (a) shows laser modified layer while micrographs (b) and (c) at Figure 3 shows the grain structure of modified layer at different depth. The focused grains were observed from top surface to the region near to HAZ in the melted pool. Found that there were changes in grain size where larger grains from top reduced to smaller grains at the end of molten pool. The microhardness found to be decreased as it moved down to substrate from top of melted pool as shown in Figure 4. This phenomenon occurred due to different cooling time. At the top of melted experienced shortest cooling time thus produced long crystalline with dendrites grain shape as shown in micrograph (b) in Figure 3. Meanwhile in micrographs (c) in Figure 3 experienced slower cooling time resulted in round grain shape. However, the grain shape elongates when approaching substrate due to rapid cooling from bulk material as shown in micrograph (d) in Figure 3.

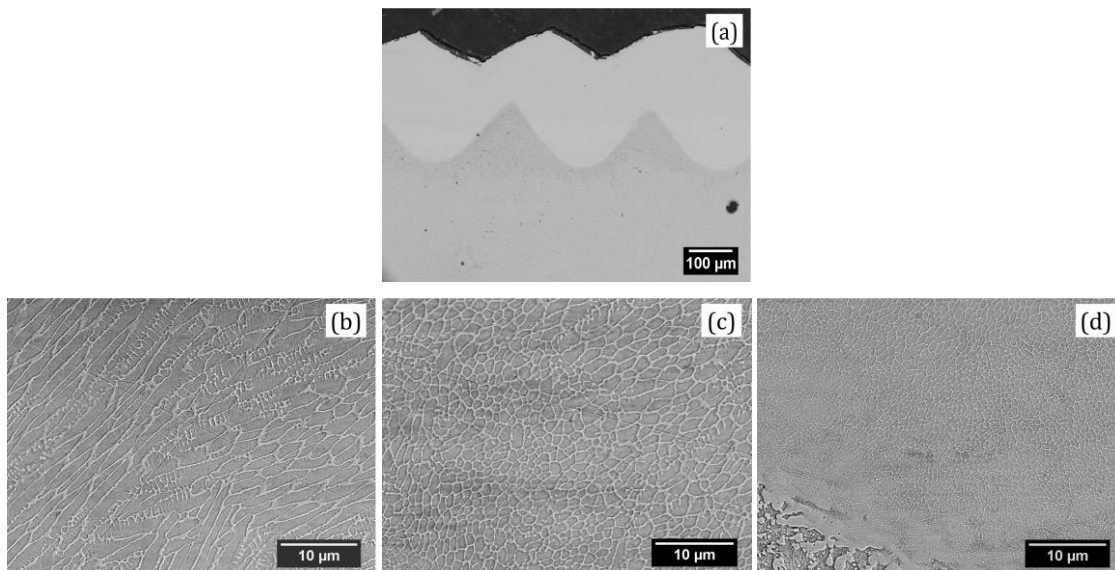


Figure 3: FE SEM micrographs of grain structure changes from top of modified layer.

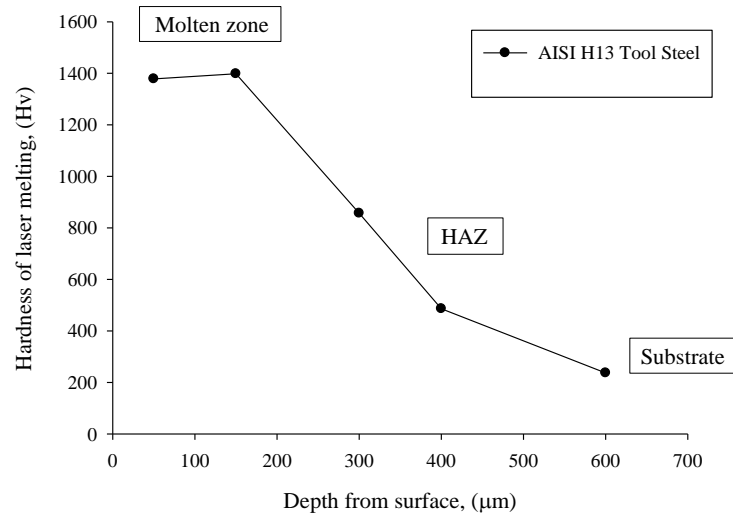


Figure 4: Hardness profile of laser modified of samples across their sectional area.

Experimental data of a full factorial  $3^3$  DOE was analyzed by response surface method (RSM) analysis using Design Expert software. The analysis of variance table (ANOVA) for all responses show significant model. Since this model statistics and diagnostic plot was found to be accepted, the model graphs were plotted by default. An example of 2D model graph of hardness response was shown in Figure 5 below. This contour plot shows the effect of interactions between peak power and PRF on the hardness response. This graph was plotted at scanning speed of 20.00 mm/s and maximum peak contour of 1162.17 Hv shows the most affected area. At peak power >2.10 kW and increasing PRF, the hardness was increased from 1162.17 Hv to maximum value of 1311.80 Hv. Decreasing peak power of <2.10 kW and increased PRF also shows increased hardness value from 1162.17 to 1236.98 Hv.

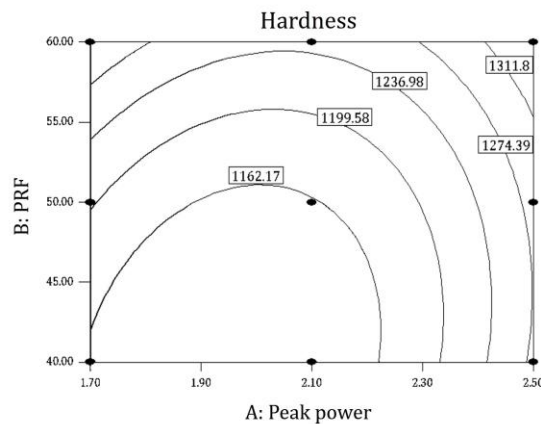


Figure 5: Hardness as function of peak power and PRF.

### 3.2 Depth of Melted Pool Properties

Power intensity also affected the laser modified depth properties. High peak power transmitted larger amount of energy which travelled deeper into substrate thus produced thick modified layer. High pulse rate also gave same effect in producing thick modified layer. The effect of irradiance on depth of laser modified layer for tool steel was studied. The effect of irradiance across residence time on depth of laser modified was plotted in Figure 6. A quadratic curve generated shows decreased laser irradiance at increasing residence time. Micrographs (a), (b) and (c) were shown in three main data point started with the highest to the lowest irradiance value. The laser modified depth of micrograph (a) with 295  $\mu\text{m}$  was generated at highest point of irradiance of 51.6  $\text{MW}/\text{mm}^2$  and  $T_R$  of  $1.03 \times 10^{-4}$  ms. While micrograph (b) with 172.5  $\mu\text{m}$  obtained at middle point at irradiance of 35.4  $\text{MW}/\text{mm}^2$  and  $T_R$  of  $1.50 \times 10^{-4}$  ms. At lowest irradiance value of 2.51  $\text{MW}/\text{mm}^2$  and  $T_R$  of  $2.16 \times 10^{-4}$  ms, the depth of modified layer generated was 79.4  $\mu\text{m}$ . Observed that depth of laser modified layer were decreased across decreasing irradiance and increased residence.

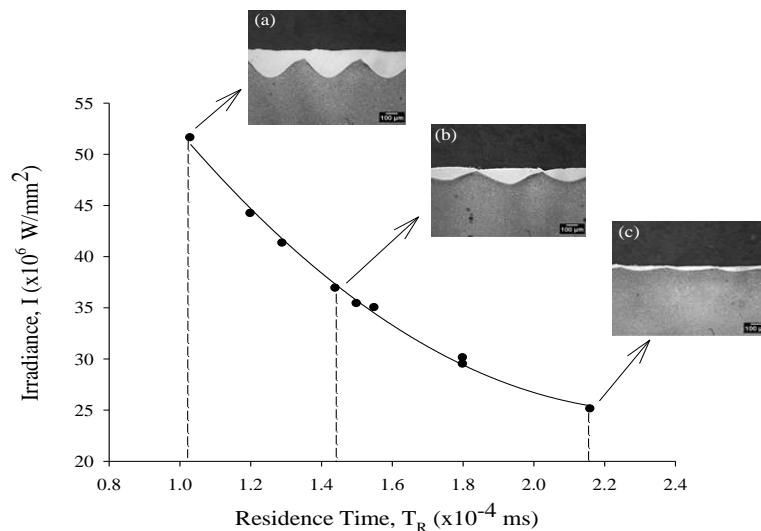


Figure 6: The plotted graph of irradiance across residence time.

Increased residence time ( $T_R$ ) prolongs the interaction time between steel surface and laser beam thus increased the depth of laser modified layer. This condition was due to increase amount of energy penetrated on the steel surface. However, micrographs shown in Figure 6 shows decrement in depth across residence time. Decreased irradiance ( $I$ ) across increased residence time affect the depth of laser modified layer as higher irradiance transmitted high energy during laser beam heating process. The higher power density allowed deep penetration of energy into the substrate and melted the surface. Thus, even though at short time interaction, high energy density laser beams capable to produce thick laser modified layer depth. Energy Dispersive X-ray Spectroscopy (EDXS) analysis of tool steel substrate was conducted to study the atomic diffusion between laser modified region with the substrate. There were five elements was recognized during analysis which included carbon (C), Silicon (Si), Chromium (Cr), Iron (Fe) and Molybdenum (Mo). The elements weight and atomic percentage were detailed in Table 3 below.

Table 3: The percentage of atomic and weight of elements in H13 substrate and modified layer.

Element	H13 substrate		H13 Laser modified	
	Weight%	Atomic%	Weight%	Atomic%
<b>C K</b>	3.49	14.23	2.28	9.64
<b>Si K</b>	0.91	1.59	0.54	0.98
<b>Cr L</b>	14.27	13.45	12.27	12.01
<b>Fe L</b>	79.55	69.81	84.91	77.36
<b>Mo L</b>	1.78	0.91		
<b>Totals</b>	100		100	

EDX analysis conducted on the laser modified surface area yields four elements of C, Si, Cr and Fe. Molybdenum (Mo) was found to be diffused after heat treated by laser treatment. Laser heating changed modified layer composition by elements diffusion of the substrate. Increased pulse energy by laser beam had increased the temperature on the surface during interaction, thus increased the atomic diffusion rate. However rapid cooling caused rapid temperature decreased on melted pool which cause the elements atom trapped in their location (Aqida, Brabazon et al. 2013). Therefore, high laser scanning speed and low overlapping spot rate could lower the percentages of elements diffusion.

Similar with other response, the contour graph of laser modified depth also was plotted at scanning speed of 20.00 mm/s. The most affected area was at highest peak contour of 306.77  $\mu\text{m}$  which is at middle of design points. At peak power of more than 2.10 kW and PRF less than 50 Hz, the laser modified layer depth decreased from 306.77 to 244.96  $\mu\text{m}$ . Similar depth decrement occurred at increased PRF from 50 to 60 Hz and more than 2.10 kW peak power. It can be concluded that the desired goal of peak laser modified depth can be achieved at centre of 2.10 kW peak power and 50 Hz PRF. The amount of energy need to melt the surface were an important parameter in producing high quality of laser modified layer. Higher laser peak power and PRF allows deep penetration on to the surface thus increased the depth of laser modified layer (Jiang, Xue et al. 2011, Sun and Hao 2012).

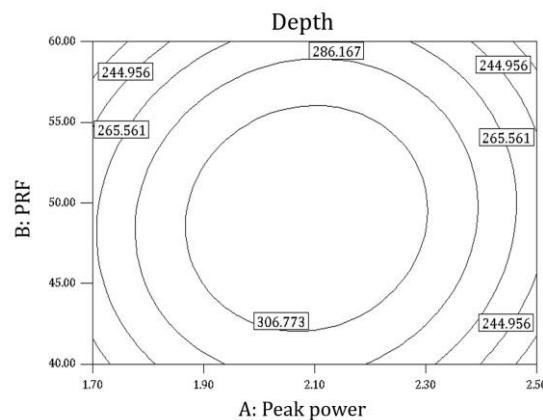


Figure 7: Hardness as function of peak power and PRF.



### 3.3 Surface roughness Properties

Surface-laser beam interaction time was essential as it controlled the surface roughness after laser modification. High scanning speed of 1400 mm/min produced low overlap percentages due to short interaction time of laser beam and sample surface. Figure 8 shows changes of overlapping laser spots at peak power range of 1.7 kW to 2.5 kW with constant PRF of 40 Hz and scanning speed ranged of 1000 to 1400 mm/min. At peak power of 1.7 kW, the overlapped laser spots in Figure 8 (a) were 30.5 %, and decreased to 16.7 % in (b) and 3.3 % in (c) increasing scanning speed. A similar pattern observed in samples with micrographs (d) to (f) and (g) to (i) at peak power of 2.0 and 2.5 kW. The overlapping rates increased with increasing peak power at constant scanning speed as shown in micrograph of Figure 8 (a), (d) and (g), which increased from 30.5 to 40.2 % and 46.3 % speed. At 1000 mm/min speed with 2.0 and 2.5 kW peak power respectively, same pattern also repeated for 1200 and 1400 mm/min scanning speed for micrographs (b), (e), (h) and (c), (f), (i). Laser beam transmitted sufficient energy on the substrate by melting the sample surface in Figure 8.

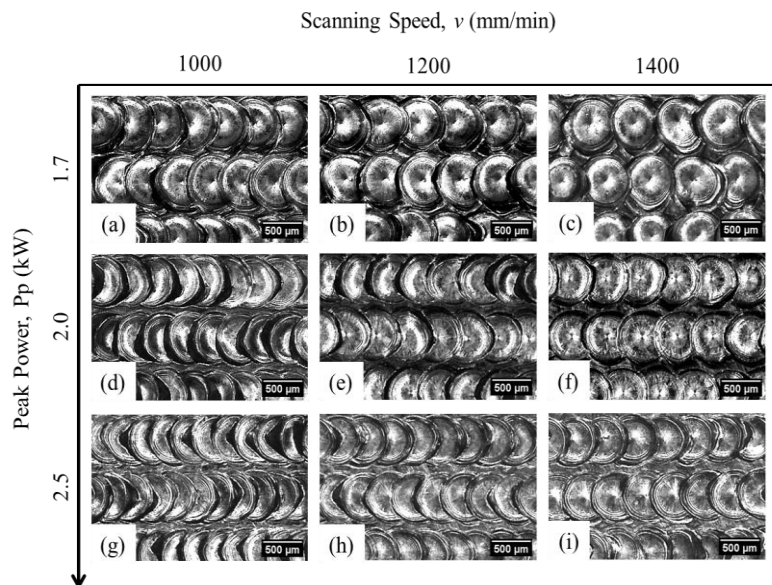


Figure 8: Micrographs of overlapping laser spots on laser modified H13 surface at scanning speed range of 1000-1400 mm/min, constant PRF of 40 Hz and peak power of (a)(b)(c) 1.7 kW, (d)(e)(f) 2.0 kW and (g)(h)(i) 2.5 kW.

The overlapping percentage increased at the higher peak power of 2.5 kW because of larger amount of energy absorbed on the surface during laser processed thus produced larger diameter spot size. This will increase the overlapping rates and surface roughness. There were three major parameters involve in this phenomenon; substrate properties, laser optics parameters and motion relation parameters. Substrate properties included initial topography, thermal and optical properties of the materials. Laser optics parameters involved were laser power, pulse duration, pulse frequency, focus length and beam shape. Motion relation parameters include speed tool, tool path trajectory, overlap percentages and number of passes (Hafiz, Bordatchev et al. 2012).

For statistical analysis, a contour plot for surface roughness is shown in Figure 9. The contour plot displays changes of roughness with peak power and PRF at constant scanning speed of 20.00 mm/s. From the ANOVA analysis, the accepted model terms were sufficient to produce quadratic model. The highest peak shows the most affected parameter setting. The maximum Ra of 9.30562  $\mu\text{m}$  was achieved at peak power ranged between 1.70 kW and 2.50 kW with PRF ranged from 43 to 55 Hz. Contour plot at PRF of less than 40 Hz and peak power of less than 2.10 kW shows decreased of surface roughness. Similar results occurred at PRF more than 55 Hz and 2.10 kW where surface roughness of 8.04347  $\mu\text{m}$  to 4.25703  $\mu\text{m}$ . Surface roughness affected at the centre of factors design points demonstrated that the data varied with the parameters. Lower PRF and peak power limited the interaction between laser beam and substrate surface thus produced lower overlapping rate. This phenomenon leads to low surface roughness due to relative flat surface produced by laser spots (Zhang, Ren et al. 2010, Hafiz, Bordatchev et al. 2012).

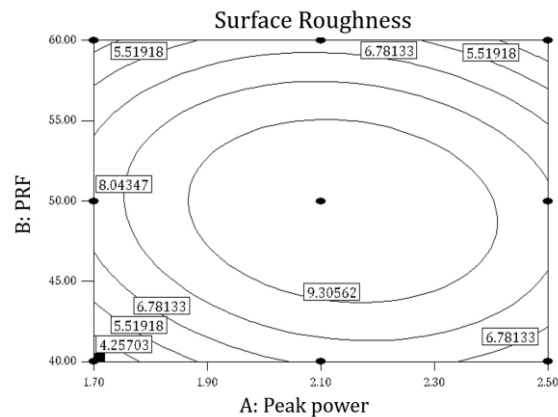


Figure 9: Contour plot of surface roughness properties responding to peak power and PRF.

### 3.4 Optimization of H13 DOE

Numerical optimization was conducted to set goals for each response and generated optimal conditions of the model. The setting parameter criteria of peak power and PRF were set in range while scanning speed with in maximum conditions. As for responses, hardness was set into maximum condition of 1427.5 Hv while surface roughness with minimum condition ranged from 1.644  $\mu\text{m}$  to 10  $\mu\text{m}$ . Depth of laser modified later response was set in range from 100  $\mu\text{m}$  to 380.37  $\mu\text{m}$ . Figure 10 depicts the desirability contour plot generated with optimal condition criteria. The contour graph was plotted across peak power and PRF at maximum scanning speed of 23.33 mm/s. The prediction value obtained was 0.906 which nearly to 1.0 indicated ideal case. Optimised predicted hardness response value was 1387.64 Hv while surface roughness with 2.7398  $\mu\text{m}$ . Depth of laser modified layer predicted value was found to be 131.667  $\mu\text{m}$ .

Optimization searches for a combination of factor levels that complied with the requirements placed on each factors and responses. Upon ANOVA analysis, the desirability prediction of 0.9 found to be in the limit range nearly to one at design point. The prediction value was the point that maximizes the desirability function. These findings signify design of materials surface modification in the many engineering applications using laser processing.

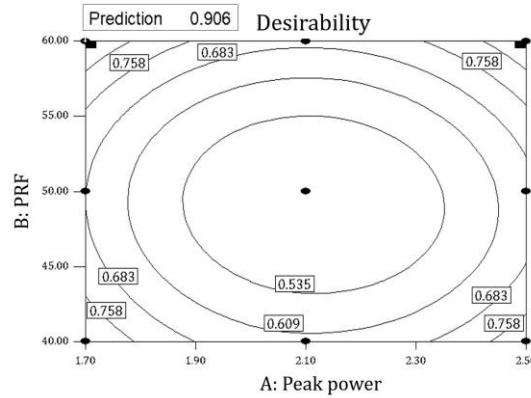


Figure 10: Desirability contour plot of H13 tool steel DOE.

### 3.5 Thermal Stability Analysis

Effect of temperature towards hardness of laser modified layer was plotted in a linear graph as shown in Figure 11. From the graph, the average hardness value of laser modified layer decreased with increasing heating temperature. The highest hardness of 1389.6 Hv decreased to 1281.3 Hv after heated with 550 °C for 15 minutes. Gradual temperature increment ranged from 600 to 800 °C resulted in decrease 50 % of the hardness properties. The hardness properties of laser modified surface decreased from 1300 to 1100.4 Hv, 960.6 Hv, 763.1 Hv, 632.7 Hv and finally 512.8 Hv when heated at respective temperature of 550, 600, 650, 700, 750 and 800 °C. A significant modified layer hardness drop was observed across the high temperature applied. High hardness of modified layer produced at high temperature generated little variation in micro-hardness most likely due to the metastable structure of laser glazed surface (Aqida, Maurel et al. 2009).

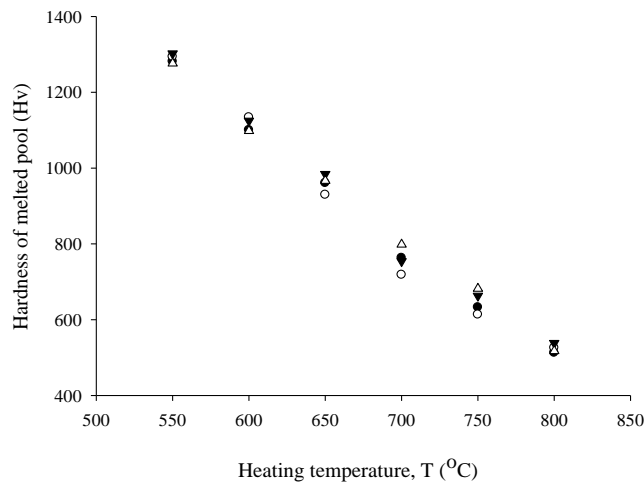


Figure 11: Hardness of laser modified layer plotted across heating temperature.

#### 4. CONCLUSIONS

This study proves laser modification as one way to enhance steel surface integrity. Finer grain microstructure of laser modified layer was analysed with average size of 0.785  $\mu\text{m}$ . The as-received substrate average grain size was 3.0709  $\mu\text{m}$ . From EDXS analysis, composition of elements changed in laser modified layer. Diffusion of elements occurred where elements C, Si, Cr, Fe and Mo shows decreased in weight after heat treatment.

The laser surface modification was successfully enhanced the hardness properties up to greater than three times higher compared to the substrate. In this study, H13 tool steel hardness obtained a maximum value of 1428 Hv which greater compared to previous works ranged from 243 to 900 Hv (Shin, Yoo et al. 2007, Hu and Yao 2008, Aqida, Naher et al. 2011, Dr. Khansaa Dawood Selman 2011). High hardness properties were due to improved parameter range in design of experiment for laser processing. The DOE was designed to meet the surface melting temperature and laser beam-surface interaction.

Significant decreased of surface roughness was achieved using DOE. Minimum surface roughness of 1.103  $\mu\text{m}$  was produced on sample 6 H13 tool steel which was processed at scanning speed, peak power and PRF of 1400 mm/min 2.5 kW and 50 Hz respectively. Applicable surface roughness range from engineering components is less than 5  $\mu\text{m}$ . The lowest overlapping rate ranged from 0 to 10 % was successfully generated at highest laser scanning speed of 1400 mm/min for all samples. Highest laser modified layer depth of 455.071  $\mu\text{m}$  was achieved on sample S4 AISI 1025 which processed at scanning speed, PRF and peak power of 1000 mm/min, 50 Hz and 2.5 kW respectively.

Design of experiment of full factorial  $3^3$  produced significant quadratic models with a fit data distribution for H13 tool steel. From ANOVA analysis, depth of laser modified layer increased with increasing peak power and laser energy density. A lower surface roughness was generated at the highest scanning speed of 1400 mm/min and a lower peak power of 1.7 kW. The hardness properties increased with increasing laser scanning speed from 1000 to 1400 mm/min.

The design optimization of H13 produced 15 solutions with the highest desirability factor of 0.906 respectively. The scanning speed and hardness was set to maximum while surface roughness was set to a range of less than 5  $\mu\text{m}$  for engineering applications. The desirability contour plot generated shows near to ideal case indicates that the model fit with the conditions.

Significant decreased of laser modified layer hardness was spotted with increasing heating temperature. The maximum hardness of 1389.6 HV<sub>0.1</sub> was decreased to 512.8 HV<sub>0.1</sub> after heated at 550, 600, 650, 700, 750 and 800 °C. A gradual temperature increment from 650 to 800 °C resulted in decreasing hardness value of almost 50 %.

#### ACKNOWLEDGEMENT

The authors gratefully acknowledge the financial support from Post Graduate Research Scheme (Grant no.: PGRS170358) and FRGS (Grant no.: RDU160141) of Universiti Malaysia Pahang.

## REFERENCES

- Aqida, S. N., Brabazon, D., & Naher, S. (2013). Atomic diffusion in laser surface modified AISI H13 steel. *Applied Physics A*, 112(1), 139-142.
- Aqida, S. N., Ahmad, S., Naher, S., & Brabazon, D. (2012). Thermal simulation of laser surface modification of H13 die steel. In *Key Engineering Materials* (Vol. 504, pp. 351-356). Trans Tech Publications.
- Aqida, S. N., Maurel, M., Brabazon, D., Naher, S., & Rosso, M. (2009). Thermal stability of laser treated die material for semi-solid metal forming. *International Journal of Material Forming*, 2(1), 761.
- Aqida, S. N., Naher, S., & Brabazon, D. (2011, May). Laser surface modification of H13 die steel using different laser spot sizes. In *AIP Conference Proceedings* (Vol. 1353, No. 1, pp. 1081-1086). AIP.
- Batista, C., Portinha, A., Ribeiro, R. M., Teixeira, V., Costa, M. F., & Oliveira, C. R. (2005). Surface laser-glazing of plasma-sprayed thermal barrier coatings. *Applied Surface Science*, 247(1-4), 313-319.
- Selman, K. D. (2011). Effect of Laser Surface Treatment on Mechanical Properties of CK45 Steel. *Engineering and Technology Journal*, 29(8), 1610-1618.
- Majumdar, J. D., Nath, A. K., & Manna, I. (2010). Studies on laser surface melting of tool steel—Part II: Mechanical properties of the surface. *Surface and Coatings Technology*, 204(9-10), 1326-1329.
- Hafiz, A. M. K., Bordatchev, E. V., & Tutunea-Fatan, R. O. (2012). Influence of overlap between the laser beam tracks on surface quality in laser polishing of AISI H13 tool steel. *Journal of Manufacturing Processes*, 14(4), 425-434.
- Hassanein, A., Sizyuk, V., Harilal, S. S., & Sizyuk, T. (2010, March). Analysis, simulation, and experimental studies of YAG and CO<sub>2</sub> laser-produced plasma for EUV lithography sources. In *Extreme Ultraviolet (EUV) Lithography* (Vol. 7636, p. 76360A). International Society for Optics and Photonics.
- Hu, Y., & Yao, Z. (2008). Overlapping rate effect on laser shock processing of 1045 steel by small spots with Nd: YAG pulsed laser. *Surface and Coatings Technology*, 202(8), 1517-1525.
- Jiang, J., Xue, L., & Wang, S. (2011). Discrete laser spot transformation hardening of AISI O1 tool steel using pulsed Nd: YAG laser. *Surface and coatings technology*, 205(21-22), 5156-5164.
- Jae-Ho, L. E. E., Jeong-Hwan, J. A. N. G., Byeong-Don, J. O. O., Hong-Sup, Y. I. M., & Young-Hoon, M. O. O. N. (2009). Application of direct laser metal tooling for AISI H13 tool steel. *Transactions of Nonferrous Metals Society of China*, 19, s284-s287.
- Roy, S., Zhao, J., Shrotriya, P., & Sundararajan, S. (2017). Effect of laser treatment parameters on surface modification and tribological behavior of AISI 8620 steel. *Tribology International*, 112, 94-102.
- Hua, M., Shao, T. M., & Tam, H. Y. (2009). Surface modification of DF-2 tool steel under the scan of a YAG laser in continuously moving mode. *Journal of Materials Processing Technology*, 209(10), 4689-4697.
- Shin, H. J., Yoo, Y. T., Ahn, D. G., & Im, K. (2007). Laser surface hardening of S45C medium carbon steel using ND: YAG laser with a continuous wave. *Journal of materials processing technology*, 187, 467-470.
- Sun, Y., & Hao, M. (2012). Statistical analysis and optimization of process parameters in Ti6Al4V laser cladding using Nd: YAG laser. *Optics and Lasers in Engineering*, 50(7), 985-995.

- Yasavol, N., Abdollah-Zadeh, A., Ganjali, M., & Alidokht, S. A. (2013). Microstructure and mechanical behavior of pulsed laser surface melted AISI D2 cold work tool steel. *Applied Surface Science*, 265, 653-662.
- Yilbas, B. S., Shuja, S. Z., Khan, S. M. A., & Aleem, A. (2009). Laser melting of carbide tool surface: Model and experimental studies. *Applied Surface Science*, 255(23), 9396-9403.
- hang, Z., Ren, L., Zhou, T., Han, Z., Zhou, H., Chen, L., & Zhao, Y. (2010). Optimization of laser processing parameters and their effect on penetration depth and surface roughness of biomimetic units on the surface of 3Cr2W8V steel. *Journal of Bionic Engineering*, 7, S67-S76.